HHS Public Access

Author manuscript

Neurobiol Dis. Author manuscript; available in PMC 2017 February 01.

Published in final edited form as:

Neurobiol Dis. 2016 February ; 86: 29–40. doi:10.1016/j.nbd.2015.11.006.

The carbonic anhydrase inhibitor methazolamide prevents amyloid beta-induced mitochondrial dysfunction and caspase activation protecting neuronal and glial cells *in vitro* and in the mouse brain

Silvia Fossati[a,1], **Patrizia Giannoni**[a,2], **Maria E. Solesio**[a,3], **Sarah L. Cocklin**[a], **Erwin Cabrera**[a], **Jorge Ghiso**[a,b], and **Agueda Rostagno**[a]

[a] Department of Pathology, New York University School of Medicine, 550 First Avenue, New York, NY 10016.

[b] Department of Psychiatry, New York University School of Medicine, 550 First Avenue, New York, NY 10016.

Abstract

Mitochondrial dysfunction has been recognized as an early event in Alzheimer's disease (AD) pathology, preceding and inducing neurodegeneration and memory loss. The presence of cytochrome c (CytC) released from the mitochondria into the cytoplasm is often detected after acute or chronic neurodegenerative insults, including AD. The carbonic anhydrase inhibitor (CAI) methazolamide (MTZ) was identified among a library of drugs as an inhibitor of CytC release and proved to be neuroprotective in Huntington's disease and stroke models. Here, using neuronal and glial cell cultures, in addition to an acute model of amyloid beta (Aβ) toxicity, which replicates by intra-hippocampal injection the consequences of interstitial and cellular accumulation of Aβ, we analyzed the effects of MTZ on neuronal and glial degeneration induced by the Alzheimer's amyloid. MTZ prevented DNA fragmentation, CytC release and activation of caspase 9 and caspase 3 induced by Aβ in neuronal and glial cells in culture through the inhibition of mitochondrial hydrogen peroxide production. Moreover, intraperitoneal administration of MTZ prevented neurodegeneration induced by intra-hippocampal Aβ injection in the mouse brain and was effective at reducing caspase 3 activation in neurons and microglia in the area surrounding the injection site. Our results, delineating the molecular mechanism of action of MTZ against Aβ-mediated mitochondrial dysfunction and caspase activation, and demonstrating its efficiency in a model of acute amyloid-mediated toxicity, provide the first combined *in vitro* and *in vivo* evidence supporting the potential of a new therapy employing FDA-approved CAIs in AD.

Corresponding authors: Silvia Fossati. [1] Department of Neurology, New York University School of Medicine, 455 First Avenue, room 823, New York, NY 10016. silvia.fossati@nyumc.org. Agueda Rostagno: [a] Department of Pathology, New York University School of Medicine, 550 First Ave, MSB 556. agueda.rostagno@nyumc.org.

[1]Present Address: Department of Neurology, New York University School of Medicine, 455 First Avenue, New York, NY 10016.

[2]Present Address: CNRS, UMR-5203, Institut de Génomique Functionnelle, Montpellier, France.

[3]Present Address: Department of Basic Sciences, New York University College of Dentistry, New York, USA.

Graphical Abstract

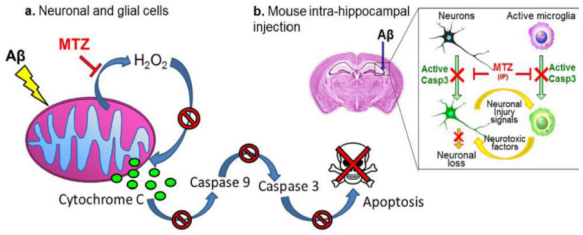

Keywords

Mitochondria; amyloid; Alzheimer's disease; carbonic anhydrase inhibitor; methazolamide; caspase activation; hydrogen peroxide; neuron; microglia; hippocampus

Introduction

Mitochondrial dysfunction has been associated with neurodegeneration and amyloid β (Aβ*) toxicity in many recent reports (Moreira et al., 2010b; Swerdlow et al., 2010), and constitutes a valuable therapeutic target for Alzheimer's disease (AD). Mitochondrial pathology and energy metabolism impairment are early events in AD patients and mouse models, preceding the formation of Aβ plaques and memory loss (Atamna and Frey, 2007; Beal, 2005; Moreira et al., 2010a; Santos et al., 2013). Recent findings in AD mice also revealed reduction in mitochondrial membrane potential (ΔΨ) and the emergence of dystrophic and fragmented mitochondria, as well as increased production of hydrogen peroxide (H_2O_2), with Aβ plaques identified as the source of toxicity (Calkins et al., 2011; Xie et al., 2013). Apoptotic cell death and caspase-3 activation have been implicated in the pathogenesis of AD. Up-regulation of pro-apoptotic proteins and DNA fragmentation were also found in the AD brain (Smale et al., 1995; Stadelmann et al., 1999). Our laboratory and others have recently shown that the release of cytochrome *c* (CytC) is one of the main events linking mitochondrial damage to caspase activation and oligomeric Aβ-mediated apoptotic cell death (Fossati et al., 2010; Fossati et al., 2013; Kim et al., 2014). Mitochondrial deregulation and the presence of CytC in the cytoplasm is often detected after acute or chronic neurodegenerative insults (Friedlander, 2003; Solesio et al., 2013a; Wang et al., 2003; Zhu et al., 2004; Zhu et al., 2002). CytC release, through activation of the "apoptosome", induces procaspase 9 proteolysis and the formation of mature caspase 9. This enzyme in turn activates caspase 3, which plays important roles in neurodegeneration, particularly in AD (de Calignon et al., 2010; Eckert et al., 2003b; Marques et al., 2003). Hence, inhibiting the release of CytC could result in protection against Aβ challenge in AD models and eventually in AD patients. A number of drugs that are able to inhibit CytC release from isolated mitochondria have been identified (Wang et al., 2008); among them, the carbonic anhydrase inhibitor (CAI) methazolamide (MTZ), proved to be neuroprotective in models of Huntington's Disease (HD) and ischemic injury (Wang et al., 2009; Wang et

*Abbreviations: Aβ = Amyloid β; AD = Alzheimer's disease; Δψ = Mitochondrial membrane potential; H_2O_2 = hydrogen peroxide; CytC = Cytochrome C; CAI = carbonic anhydrase inhibitor; MTZ = methazolamide; HD = Huntington's disease; ROS = reactive oxygen species; IP = intraperitoneal; DR = death receptor

al., 2008). A striking correlation was found between MTZ treatment and the preservation of $\Delta\Psi$ across the inner mitochondrial membrane, in HD models as well as in our previous studies on vascular and neuronal amyloid toxicity (Fossati et al., 2013; Wang et al., 2008). Of note is that this drug has been used in humans for many years for treatment of glaucoma and can easily cross the blood brain barrier. Moreover, CAIs are clinically used for the prevention of acute mountain sickness and related high-altitude cerebral edema, confirming the efficacy of the drugs in the brain and the safety of their systemic administration (Wright et al., 2008). Here, we studied the effects of MTZ on caspase activation and apoptosis induced by Aβ challenge in neuronal and glial cells through the modulation of CytC release and mitochondrial H_2O_2 production. Moreover, we analyzed the influence of MTZ on caspase 3 activation and neurodegeneration induced by Aβ after intra-hippocampal injection in the mouse brain. Our results provide *in vitro* and *in vivo* evidence highlighting the potential of pharmacological strategies employing MTZ as promising new therapeutic avenues to explore in AD.

Materials and Methods

Aβ Peptides

Synthetic homologues of the amyloid subunits Aβ42 and Aβ40-Q22 (the Dutch genetic variant, containing the E22Q substitution) were synthesized using *N-tert*-butyloxycarbonyl chemistry by James I. Elliott at Yale University. Aβ homologues were dissolved to 1 mM in 1,1,1,3,3,3-hexafluoro-2-propanol (HFIP; Sigma), incubated overnight to break down pre-existing β-sheet structures (Fossati et al., 2010), and lyophilized. Peptides were subsequently dissolved in DMSO to a 10 mM concentration, followed by the addition of deionized water to 1 mM concentration and by further dilution into culture media to the required concentrations for the different experiments.

Cell cultures

Human neuroblastoma cells (SH-SY5Y) were obtained from the American Type Culture Collection (ATCC, Manassas, VA, USA) and maintained in DMEM/F12 medium (50:50, Mediatech, Manassas, VA) with 10% FBS. M059K Glioma cells were obtained from ATCC and maintained in DMEM with 10% FBS. Normal Human Astrocytes were purchased from Lonza (Walkersville, MD) and were cultured in Astrocyte Growth Medium (Lonza) containing the pertinent growth factors and FBS provided by the manufacturer.

Cell death ELISA

The extent of apoptosis caused by Aβ in presence or absence of MTZ was assessed by quantitation of nucleosome formation using Cell Death ELISA^{plus} (Roche Applied Science, Indianapolis, IN). Briefly, after incubation with the peptides, plates were centrifuged in a Beckman J-6B centrifuge (10 min; 1,000 rpm), cells lysed, and DNA-histone complexes (nucleosomes) quantitated by Cell Death ELISA, as previously described (Fossati et al., 2010).

Thioflavin T binding assay

Binding of the different Aβ peptides to Thioflavin-T was monitored by fluorescence evaluation, as described (Fossati et al., 2010; Walsh et al., 1999). Briefly, after peptide aggregation at 50 μM concentration in culture media in presence or absence of MTZ, 6 μl aliquots from each of the time-points were added to 184 μl of 50 mM Tris-HCl buffer, pH 8.5, and 10 μl of 0.1 mM Thioflavin-T (Sigma). Fluorescence was recorded for 300s in a LS-50B luminescence spectrometer (Perkin Elmer, Waltham, MA) with excitation and emission wavelengths of 435 and 490 nm (slit width 10 nm), respectively, as described (Solito et al., 2009; Viana et al., 2009).

Native gel electrophoresis and Western blot analysis

Electrophoretic analysis for assessment of peptide aggregation in presence or absence of MTZ was performed under native conditions using 5–30% gradient polyacrylamide gels, in absence of SDS, using 25 mM Tris/glycine, pH 8.8, as running buffer, as previously described (Fossati et al., 2010). Aβ oligomerization patterns were visualized by subsequent WB analysis. Briefly, proteins were electrotransferred to nitrocellulose membranes (0.45 μM pore size; Hybond-ECL, GE Healthcare Life Sciences, Piscataway, NJ) at 400 mA for 2.5 h, using 10 mM 3-cyclohexylamino-1-propanesulfonic acid (CAPS; Sigma) buffer, pH 11.0, containing 10% (v/v) methanol. After blocking with 5% nonfat milk in TBS containing 0.1% Tween 20 (TBST), membranes were immunoreacted with a combination of mouse monoclonal anti-Aβ antibodies 4G8 (epitope: residues Aβ18-22) and 6E10 (epitope: residues Aβ3-8), both from Covance (Princeton, NJ), at 1:3000 dilution each, followed by HRP-labeled anti-mouse IgG and ECL chemistry (Fossati et al., 2010).

Immunocytochemical evaluation of CytC release

Both SH-SY5Y cells and Glioma cells were plated on glass chamber slides (Thermo Fisher Scientific, Rochester, NY). Slides were pre-coated with poly-D-lysine for SH-SY5Y cells. After seeding, cells were allowed to attach for 1 day prior to treatment with Aβ in presence or absence of MTZ for 24 hours. Cells were then washed with PBS, fixed with 4% paraformaldehyde (10 min, RT), washed again, and blocked for 1 hour with 20 mg/ml BSA in PBS containing 0.3% Triton X-100 (PBST). Slides were further incubated with mouse monoclonal anti-CytC antibody (BD Biosciences; 1:200 in PBST containing 5 mg/ml BSA; 2h, RT) followed by Alexa Fluor 488-conjugated anti-mouse IgG (Life Technologies, Grand Island, NY) 1:200 in PBST with 5 mg/ml BSA for 1h at RT, as previously described (Fossati et al., 2013). Fluorescence signals were visualized in a Zeiss LSM 510 laser scanning confocal/Confocor2 microscope using a 40x DIC oil immersion objective and LSM 510 software; acquired images were processed and analyzed using ImageJ (National Institute of Health; http://rsbweb.nih.gov/ij/).

ELISA and Western blot assessment of CytC in mitochondrial and cytoplasmic subcellular fractions

Subcellular distribution of CytC in amyloid-challenged SH-SY5Y and glioma cells was determined in mitochondrial and cytoplasmic protein extracts prepared using Mitochondria Isolation Kit (MITOISO2, Sigma) following the manufacturer's specifications. Briefly, after

amyloid challenge in presence and absence of Methazolamide, as above, cells were collected by trypsinization, resuspended in 10 mM HEPES, pH 7.5, containing 200 mM mannitol, 70 mM sucrose, 1 mM EGTA and Protease Inhibitor Cocktail, and homogenized with the aid of a Dounce glass homogenizer. Cell homogenates were centrifuged to remove unbroken cells and nuclei (600 × g, 5 min, 4°C) and supernatants were further centrifuged at 11,000 × g (5 min, 4°C) to subfractionate mitochondria. Supernatants, representing the cytosolic fractions as well as mitochondrial fractions were analyzed by CytC ELISA and WB.

a) Solid phase ELISA—The concentration of CytC in cytosolic and mitochondrial fractions was quantitated by solid phase sandwich ELISA (Quantikine ELISA, human Cytochrome C Immunoassay, R&D Systems) as described by the manufacturer. Prior to the assay, fractions containing cytoplasmic proteins were concentrated on Vivaspin 500 centrifugal concentrators (GE HealthCare, molecular weight cut off 5000), mitochondrial pellets were resuspended in Cell Lysis Buffer provided with the kit, and total protein of the respective fractions was evaluated by BCA protein assay (Thermo Fisher Scientific/Pierce). Samples and human CytC standards were diluted in Calibrator Diluent and incubated with microtiter wells pre-coated with a monoclonal antibody specific for human CytC. After washing away unbound proteins, wells were further incubated with an HRP-linked monoclonal antibody anti-human CytC, color developed with tetramethylbenzinine peroxidase substrate, and evaluated through quantitation of the Absorbance at 450 nm. The CytC concentration of the different samples was interpolated from the standard curve with the aid of GraphPad Prism and normalized to the protein content of the respective subcellular fractions.

b) Western blot analysis—Cytosolic and mitochondrial fractions were separated on 14% SDS-polyacrylamide gels under reducing conditions and electrotransferred to PVDF membranes (Immobilon, Millipore, Billerica, MA; 0.45 μm pore; 400 mA, 1.5h) using CAPS buffer, as above. Membranes were blocked with 5% nonfat milk in TBST, and subsequently immunoreacted with mouse monoclonal anti-CytC antibody (BD; 1 μg/ml in 5 % nonfat milk in TBST, overnight, 4°C) followed by HRP-labeled anti-mouse IgG (1:10,000; GE Healthcare), and ECL detection, as above. As loading controls, membranes were probed with rabbit polyclonal anti-β actin (Novus Biologicals; 1 μg/ml, overnight, 4°C) followed by HRP-labeled anti-rabbit IgG (1: 5,000; GE Healthcare). Densitometric assessment of band intensities was performed using ImageJ software (rsbweb.nih.gov)

Caspase 9 and caspase 3/7 activity assay

Caspase 9 and caspase 3/7 activation were measured by luminescent assays (Caspase-Glo 9 and caspase-Glo 3/7, Promega, Madison, WI), in cells treated with the Aβ peptides in DMEM without FBS. Briefly, 10.000 cells/well were plated in white 96 wells plates and incubated for 24 hours with the freshly solubilized Aβ peptides. Caspase-Glo reagent was added to the cell cultures resulting in cell lysis, followed by caspase cleavage of the substrate and generation of a luminescent signal produced by the luciferase reaction. After 60 minutes incubation, the amount of caspase activity was evaluated in a plate-reading luminometer (Synergy HT Multi-Mode Microplate Reader, Biotek, Winooski, VT) as described in (Fossati et al., 2012b). To inhibit non-specific background activity, the

proteasome inhibitor MG-132 was added to the Caspase-Glo reagent before the experiment as indicated by the manufacturer. In all cases results are expressed as fold-change compared to untreated control cells.

Immunocytochemical evaluation of active Caspase 3

SHSY-5Y and Glioma cells were plated on chamberslides as above. Slides were pre-coated with Poly-D-Lysine 30 μg/ml for 2 hours for SHSY-5Y cells. Cells were treated with Aβ peptides in presence or absence of MTZ (100 or 300 μM), and stained, as above, with a rabbit monoclonal antibody against the activated form of Caspase 3 (Cell Signaling Technology, Danvers, MA), followed by Alexa Fluor 488-conjugated anti-rabbit IgG (Life Technologies; 1:200 in PBST with 5 mg/ml BSA; 1 h, RT). Nuclei were counterstained in blue with DAPI. Images were acquired using a Nikon Eclipse Ti inverted microscope with a 20X objective, and NIS Elements software.

Mitochondrial H_2O_2 production

Production of H_2O_2 in isolated mitochondria was measured using Amplex Red Hydrogen Peroxide/Peroxidase Assay (Life Technologies). Cells were treated with Aβ peptides, in presence or absence of MTZ. After 16 hours of treatment, the mitochondrial fraction was separated from nuclear and cytoplasmic fractions as previously described (Fossati et al., 2013). Protein concentration in the mitochondrial fraction was measured by BCA assay (Thermo Scientific, Rockford, IL), in order to include the same amount of mitochondria in each sample. Functional mitochondrial fractions were distributed in a 96-well plate with Reaction Buffer and Amplex Red solution following the manufacturer's specifications. The plate was incubated in the dark at room temperature for 30 minutes before colorimetric evaluation of the Amplex Red reaction at 560 nm.

Cellular ROS Measurement

SH-SY5Y and glioma cells were seeded at a density of 10^4 cells/well on 96-well plates and challenged with Aβ in presence or absence of MTZ for 16h. For the last 30 minutes, the cells were incubated in the experimental medium at 37 °C with 5 μM CellROX Deep Red (Life Technologies) and 1 μg/ml Hoechst Stain (Immunochemistry Technologies, Bloomington, MN), as described by the manufacturer, followed by washes. Fluorescence was measured using a FlexStation 3 Multi-Mode Microplate Reader (Molecular Devices, Sunnyvale, CA).

Hippocampal injections with Aβ peptide

Six months old C57BL/6 mice were anesthetized with a mixture of ketamine and xylazine (120 and 10mg/Kg respectively) i.p. and fixed to a stereotaxic frame (David Kopf Instruments, Tujunga, CaliforniaKopf). The body temperature was maintained stable with the use of a heating pad (Harvard Apparatus, Holliston, MA) for the total time of the surgery. A volume of 1μl of a 10μM fresh solution of Aβ40-Q22 - chosen for its propensity to form toxic oligomers, and not fibrils, in the first few hours after solubilization - (Fossati et al., 2010) in PBS, or the vehicle for control mice, was injected in the hippocampus (Coordinates: AP=−2.7, L=−3.0 and H=−4.0, according to the Atlas of Paxinos and Franklin) at a flow rate of 0.1μl/min. The needle (Hamilton 701 RN 10μl syringe, RN needle

30/2”/3S) was left in place for two minutes and then slowly withdrawn. In the cases in which MTZ treatment was administered, mice were injected intraperitoneally with a solution of MTZ (20 mg/kg) 1h before the Aβ40-Q22 intrahippocampal injection. At the selected time after injections, the animals were sacrificed by trans-cardiac perfusion (medium flow pump, Fisher Scientific 13-876-2, 10ml/min flow rate) with PBS for 2 minutes followed by 4% paraphormaldehyde for 5 minutes. Brains were then removed from the skull and postfixed in 4% paraphormaldehyde for 2h at 4°C. Cryoprotection was achieved with a solution of sucrose 15% for a day, later changed to a solution of sucrose 30% for 2 days. Brains were then washed in PBS, assembled in a plastic mold with Tissue-Tek O.C.T. compound (Fisher Scientific), and frozen with a mixture of liquid nitrogen and isopenthanol. Serial cryostat sections of 8μm thickness were collected on positively charged microscope slides (Fisher Scientific) and stored at −80°C until further immunohistochemical analysis.

Immunohistochemistry

For immunohistochemical staining, slices were warmed to RT for 5’ prior to use, rinsed in PBS and blocked with Mouse on Mouse (MOM) blocking reagent (2 drops in 2.5 ml of PBS, Vector Laboratories, Burlingame, CA) for 20 minutes. Incubation with the rabbit monoclonal antibody against active caspase-3 (Cell Signaling Technology) was performed overnight at 4°C in PBS containing 0.1% triton X-100 and 5 mg/ml BSA. The day after, the sections were washed three times with PBS and incubated in Alexa Fluor 488- or 633-conjugated anti-rabbit IgG (Life Technologies; 1:200 in PBST with 5 mg/ml BSA; 1h at RT), followed by primary anti-Aβ 6E10 (1:200 in PBS + MOM for 2 hours at RT), and by secondary Alexa Fluor 568 anti-mouse IgG. Finally, the slices were washed and the DNA counterstained with TO-PRO (Life Technologies) 1:1000 for 10 min, or with NeuN green neuronal staining (1:100 in PBS for 1 hour, Millipore, Temecula, CA). For staining of active microglial cells, tissue sections were incubated with anti IBA1 goat antibody (Abcam, Cambridge, MA) 1:200 in PBS containing 0.1 % Triton and 5mg/ml BSA for 1 hour, followed by Alexa Fluor 488 anti-goat IgG (1 hour). After washing, slides were mounted with an aqueous mounting medium (Vector Laboratories). Images were acquired in a Zeiss LSM 510 confocal microscope using 40x or 100x oil lens and processed using Image J and Adobe Photoshop. Images were acquired maintaining constant exposure for all samples across single experiments. For IF signal quantifications, stained brain slices corresponding to the injection site area of 3 or more animals were analyzed with Image J. The total area of NeuN, caspase 3, Aβ and IBA1 positive cells was quantified and compared between different treatments.

Statistical Analysis

ANOVA with Tukey post hoc tests for comparison of multiple groups and unpaired t test for comparison of 2 groups were performed using GraphPad Prism (GraphPad, La Jolla, CA). Values of $P \leq 0.05$ were considered significant.

Results

MTZ prevents neuronal and glial Aβ-mediated apoptosis without affecting peptide aggregation

Treatment with different familial or sporadic variants of Aβ has been shown to induce apoptosis in multiple brain cell types, including neuronal and glial cells (Bashir et al., 2014; Fossati et al., 2013; Modi et al., 2014). We therefore challenged neuronal SHSY-5Y cells, M059K glioma cells and Normal Human Astrocytes with WT-Aβ42 (10 μM), and the Dutch mutant of Aβ40 (Aβ40-Q22, 50 μM). While Aβ40 is typically less toxic for neuronal cells compared to Aβ42, the Aβ40-Q22 variant is known have a high propensity to form toxic oligomers after very short aggregation times (Cruz et al., 2005; Fossati et al., 2010; Fossati et al., 2012a), and to affect synaptic structure in AD mouse models (Price et al., 2014). In our hands, both Aβ42 and Aβ40-Q22 caused an increase of 2 to 3 times in the level of apoptosis, measured as amount of fragmented DNA by Cell death ELISA^{PLUS}, for all the cell types analyzed (Figure 1a). The CAI MTZ was able to significantly reduce the number of fragmented nucleosomes after challenge with Aβ42 and Aβ40-Q22 in both neuronal and glial cells, consistent with our previous findings in brain endothelial and smooth muscle cells (Fossati et al., 2010), as well as with the ability of MTZ to rescue neuronal cells in Huntington's and stroke models (Wang et al., 2009; Wang et al., 2008). The effect of 300μM MTZ completely prevented the Aβ-mediated increase in fragmented nucleosomes for all the cell types challenged with Aβ42, and for both neuronal and glioma cells treated with Aβ40-Q22. MTZ at 100 μM concentration was also significantly effective at reducing DNA fragmentation, and completely reverted the apoptotic phenotype caused by the Aβ peptides in glioma cells.

In order to rule out the possibility that the protective effect of MTZ could be due to a decrease in Aβ aggregation propensity in presence of the drug, we tested the formation of different aggregation species *in vitro* in the presence or absence of MTZ. When the peptides were aggregated for up to 3 days at the same concentration and in the same media used for the cell experiments in presence of 100 or 300μM MTZ, we did not find any significant difference in fibrillization, as evaluated by Thioflavin T fluorescence (Figure 1b). Furthermore, the aggregation species yielded by both Aβ42 and Aβ40-Q22 in presence or absence of the CAI at the respective time points did not differ as evaluated by electrophoretic separation of the aggregated peptides in native gels and immunoreaction with anti-Aβ antibodies (Figure 1c).

Cytochrome C release, caspase 9 and caspase 3 activation are prevented by MTZ through the inhibition of mitochondrial H_2O_2 production

It is currently recognized that mitochondrial dysfunction is an early event in AD patients and in AD mice models, preceding and inducing the activation of caspases and the neurodegenerative process (Atamna and Frey, 2007; Balietti et al., 2013; Calkins et al., 2011; Du et al., 2010). We have previously shown how Aβ genetic variants trigger common mitochondria-mediated cell death pathways within different time frames, correlating with the aggregation properties of each peptide (Fossati et al., 2010; Fossati et al., 2012b; Fossati et al., 2013). Since CytC release is a common pathological event linking mitochondrial

dysfunction to apoptotic cell death, we asked whether MTZ was able to inhibit Aβ-induced CytC release in neuronal and glial cells. CytC staining, visible as chain-like structures representing mitochondrial localization of the molecule in healthy cells, was diffused in the cytoplasm after cell incubation with Aβ42 10μM for 24 hours. This indicates release of the molecule from the mitochondrial inter-membrane space, a typical point of no return in both the extrinsic and intrinsic apoptotic pathways. In presence of 100μM MTZ given together with Aβ, the release of CytC was prevented in both neuronal and glial cells (Figure 2). The release of CytC in Aβ-treated SHSY-5Y and glioma cells and its inhibition by MTZ were also confirmed by CytC ELISA and Western blot performed in mitochondrial and cytosolic fractions, as shown in Figure 3. Since CytC release is known to be an essential event for the maturation and activation of caspase 9 through formation of the apoptosome (Jiang and Wang, 2000; Kim et al., 2005), we tested whether caspase 9 activation, typically induced by Aβ, as previously shown (Fossati et al., 2012a; Fossati et al., 2012b; Zussy et al., 2013), could be inhibited by MTZ. As expected, when both neuronal and glial cells were challenged with 10μM Aβ42 for 24 hours, caspase 9 activation, measured by luminescence, was significantly increased (about 1.5 times) compared to control cells (Figure 4a). Caspase 9 over-activation was completely inhibited in presence of 100 or 300μM MTZ in neuronal cells, and was significantly reduced in glial cells. MTZ alone in absence of Aβ, used as a control, did not have any effect on caspase 9 activity. Importantly, caspase 3 - the executioner caspase, activated by caspase 9, and capable of inducing synaptic dysfunction and Tau tangle formation in the AD brain (D'Amelio et al., 2011; de Calignon et al., 2010) - was also activated after Aβ challenge in neuronal and glial cells, as indicated by the green fluorescence shown after immunostaining of active-caspase 3 in Figure 4c.

As for caspase 9, active-caspase 3 staining and activity of caspases 3/7 measured by luminescence (Figure 4d), were greatly suppressed when Aβ was co-incubated with MTZ at both concentrations, suggesting a protective effect of the CAI on the downstream neurotoxic effects of Aβ, known to be mediated by these proteases (Burguillos et al., 2011; D'Amelio et al., 2011). Since caspase activation, as well as neuronal and glial dysfunction, are often induced by overproduction of mitochondrial and cellular reactive oxygen species (ROS), we tested weather MTZ affected cellular and mitochondrial Aβ-mediated ROS production.

After 24 hours treatment with Aβ42 in presence or absence of MTZ, the levels of cellular ROS in neuronal SHSY-5Y and glial cells, measured by fluorescence of the ROS indicator CellROX inside the cells, did not significantly change, albeit 25μM Aβ42 induced a slight increase in neuronal cells (not shown). Intriguingly, when we analyzed the levels of H_2O_2 produced by isolated mitochondria after treatment with Aβ in presence or absence of MTZ, we found a significant increase in H_2O_2 production by the mitochondria of Aβ-challenged cells, which was completely reverted by MTZ for both neuronal and glial cells (Figure 4b). MTZ alone did not have any effect on H_2O_2 production in untreated cells. Notably, H_2O_2 is the only ROS that can function directly as a second messenger in a physiologically relevant manner (Ding et al., 2008; Forman et al., 2004; Gill and Levine, 2013; Lee et al., 2011), and has been shown to be directly responsible for the release of CytC from the mitochondria as well as for the activation of caspase-3 and neuronal apoptosis in other models of neurodegenerative disease (Saito et al., 2007; Solesio et al., 2013b; Zhou et al., 2014), suggesting that the prevention of mitochondrial H_2O_2 production observed in presence of

MTZ may also be associated with the ability of the drug to inhibit CytC release and reduce caspase activation in our model.

Hippocampal caspase 3 activation and neurodegeneration caused by injected Aβ are inhibited by MTZ

Injection of oligomeric forms of Aβ in the rodent brain has been shown to provoke long-lasting pathological alterations comparable to the human disease, including caspase activation and neuronal loss (Zussy et al., 2013). We analyzed Aβ-induced caspase activation *in vivo* using a stereotaxic procedure to deliver Aβ in the hippocampus of wild-type mice, as an *in vivo* correlate of interstitial Aβ accumulation. Figure 5a shows the site of injection in the CA3 region of the hippocampus (left panel) and the post-injection localization of the peptide, which was found in the brain parenchyma as well as intracellularly 1 hour after inoculation (right panel). Synthetic Aβ42 is known to form insoluble fibrils very early after solubilization (Chang and Chen, 2014; Fossati et al., 2010), forming in proportion fewer oligomers, which are recognized to be the toxic species responsible for caspase activation and synaptic failure. In light of this, we chose to inject Aβ40-Q22, which was shown to form a high level of oligomers after a few hours aggregation, and could persist in oligomeric form for a longer time after injection in the mouse brain compared to Aβ42 (Fossati et al., 2010). In our model, Aβ40-Q22 specifically induced caspase-3 activation in the hippocampus of mice sacrificed 4 hours after injection. Interestingly, we observed that caspase 3 was activated specifically only in the neurons containing internalized peptide in the CA1 hippocampal region contiguous to the site of injection (Figure 5b, 40X magnification in the top panels, 100X in the bottom). Importantly, the activation of caspase-3 induced by Aβ in CA1 neurons was prevented by systemic intra peritoneal (IP) administration of 20 mg/Kg MTZ, as shown in Figure 6. Neurons stained with NeuN and containing internalized Aβ were positive for active caspase 3 in mice injected with the peptide alone, but were negative for the active caspase when the mice were treated systemically with MTZ 1 hour prior to peptide injection. Furthermore, analyzing the area of the hippocampus immediately adjacent to the CA3 injection site, at a distance from the trace of injection of ≤ 100 μm (Figure 7, top panels), we observed a high amount of intracellular and parenchymal Aβ coexisting with high caspase 3 activation and loss of neuronal NeuN staining, when compared to the corresponding area in the contralateral hippocampus (Figure 7, middle panels). Loss of NeuN staining has been associated with oxidative stress, neuronal mitochondrial damage and acute neurotoxicity in many reports (Choi et al., 2005; Duffy et al., 2011; Wu et al., 2010), and suggests neurodegeneration in the vicinity of the Aβ injection site. Importantly, in mice treated IP with MTZ one hour before peptide injection (bottom panels), loss of NeuN immunoreactivity and caspase activation in the vicinity of the injection site were significantly reduced, as indicated by quantification of IF signals for NeuN, active caspase 3 and Aβ staining illustrated in Figure 9a. Overall, our results indicate that MTZ, when administered systemically, can enter the mouse brain and is effective in preventing Aβ-induced caspase activation and neurodegeneration in an acute *in vivo* model of amyloid toxicity, at concentrations consistent with those used in animal models of Huntington's and muscular dystrophy (Giacomotto et al., 2009; Wang et al., 2008) and with the human doses of CAIs.

MTZ prevents caspase 3 activation in active microglial cells containing internalized Aβ

Activated microglial cells, the resident immune cells of the central nervous system, play prominent roles in the pathogenesis of neurodegenerative disorders, including AD. However, uncontrolled and over-activated microglia can trigger neurotoxicity (Burguillos et al., 2011). In the mature brain, microglial cells typically exist in a resting state characterized by a ramified morphology. In response to certain cues such as brain injury or immunological stimuli, they are readily activated and undergo a dramatic transformation from their resting ramified state into an amoeboid morphology (Block et al., 2007). Recent reports indicate that microglial activation is capable of both initiating additional neuronal loss and amplifying ongoing neuronal damage, indicating that microglia might be crucial to the etiology and the progressive nature of neurodegenerative diseases. Microglial activation in cell and animal models of inflammation involves caspase activation, and inhibition of the cascade in microglia prevents neurodegeneration. Accordingly, significant cytoplasmic expression of active caspase-3 was found in microglial cells of postmortem AD brains, compared with controls (Burguillos et al., 2011). Here we analyzed the presence of active caspase 3 in microglia activated by Aβ injection. After injection of Aβ in presence or absence of MTZ, a similar number of Aβ-positive cells around the injection site presented IBA1 staining, indicative of microglial activation (Figure 8). While cells positive for both IBA1 and Aβ presented high active-caspase 3 fluorescence in mice injected with only Aβ (top panels, arrows), active-caspase 3 staining was notably lower in mice that were previously given IP injections of MTZ (bottom panels, arrowheads), as confirmed by the yellow color of these cells in the merged image, compared to the white color in absence of MTZ. Quantification of the area exhibiting staining for active caspase 3, IBA1, as well as their ratio in microglial cells at the injection site, are illustrated in Figure 9b and demonstrate a significant decrease of caspase 3 activation in microglia in presence of MTZ. The ability of MTZ to decrease caspase 3 activation in reactive microglia is indicative of a protective effect of the compound not only towards glial cell death and the toxic effects of an excessive inflammatory reaction, but also against the microglia-mediated amplification of the neurodegeneration process.

Discussion

Here, we report that Aβ-induced neuronal and glial mitochondrial dysfunction, caspase activation and apoptotic cell death can be prevented by the CAI MTZ. Our studies demonstrated that release of CytC and activation of both caspase 9 and the effector caspase 3 caused by Aβ challenge were prevented by MTZ in neuronal and glial cells in culture and in the mouse brain. MTZ was also able to hinder terminal DNA fragmentation - indicative of apoptotic cell death - in both cell types, without affecting the peptides aggregation patterns. Moreover, we showed that the primary mechanism of action of MTZ involves the inhibition of mitochondrial H_2O_2 production and the subsequent prevention of mitochondrial degeneration and CytC release in both cell types. Importantly, after intra-hippocampal Aβ injection in the mouse brain, which resulted in cellular uptake of the peptide and activation of caspase 3 in neurons and microglia, administration of MTZ was able to prevent neuronal and glial caspase activation as well as hippocampal neuronal loss.

Mitochondrial dysfunction and loss of ΔΨ are known as early events in the AD pathology (Balietti et al., 2013; Eckert et al., 2003a; Swerdlow et al., 2010), preceding the activation of caspases and memory loss (Atamna and Frey, 2007; Beal, 2005), and constituting a valuable therapeutic target for AD research (Moreira et al., 2010a; Moreira et al., 2010b). Mounting evidence suggests a role for the activation of caspases in the AD brain and proposes that this event may occur through stimulation of death receptor (DR) pathways by Aβ oligomeric species. Our recent work demonstrated that oligomers and protofibrils of WT-Aβ40, as well as its vasculotropic mutants, engaged DRs activating caspase 8 and 9 and inducing mitochondrial dysfunction, with loss of ΔΨ and CytC release in cerebral endothelial and neuronal cells in culture (Fossati et al., 2010; Fossati et al., 2012a; Fossati et al., 2012b; Fossati et al., 2013). The possibility of blocking early mitochondrial damage in the brain using CAIs, reducing production of mitochondrial ROS, and the resulting release of CytC and activation of caspases, could represent an interesting approach in both prevention and therapy for AD. Interestingly, recent *in vivo* findings have shown that caspase activation triggers early synaptic dysfunction in AD mouse models (D'Amelio et al., 2011). Active caspases also cleave Tau to initiate tangle formation in Tau transgenic mice (de Calignon et al., 2010). Therefore, the preservation of healthy mitochondria is a key factor not only to prevent energetic failure in the AD brain, but also to inhibit the activation of caspases, such as caspase 9 and 3, thereby preventing synaptic dysfunction, tangle formation and the resulting neurodegeneration.

Importantly, our study represents the first evidence of a protective effect of a CAI against amyloid challenge in the mouse brain. Carbonic anhydrases (CAs) are a family of enzymes catalyzing the conversion of CO_2 to bicarbonate and protons. They have a role in a number of physiological processes such as diuresis, production of body fluids, gluconeogenesis and lipogenesis. Sixteen mammalian isozymes have been discovered, among which CA VA and CA VB are mitochondrial. Several CAIs, among them MTZ, have high activity against mitochondrial CA. CAIs exhibit numerous beneficial effects, among others they have been shown to increase cerebral blood flow (Grossmann and Koeberle, 2000), decrease extracellular pH in the brain inducing vasodilation (Bickler et al., 1988), and increase neuronal excitability and visual processing (Aamand et al., 2011). All these characteristics could prove fundamental for an additional neuroprotective effect in AD. Noteworthy, CAIs are safe, have been used chronically for many years against glaucoma, and can easily cross the blood brain barrier. CAIs such as acetazolamide (well tolerated in humans up to a 1000 mg daily dose) are also currently FDA-approved for the prevention of acute mountain sickness and related high-altitude cerebral edema, confirming the efficacy of this and analog sulfonamides in the brain and the safety of their systemic administration (Wright et al., 2008). Their possible application in preventing/ameliorating neurodegeneration is also supported by the neuroprotective effects of MTZ in cellular and animal models of Huntington's disease (HD) and stroke (Wang et al., 2009; Wang et al., 2008), and by the ability of CAIs to inhibit high glucose induced ROS production and apoptosis in cerebral perycites (Shah et al., 2013a; Shah et al., 2013b).

Remarkably, our data shows for the first time that MTZ is effective at inhibiting the overproduction of mitochondrial H_2O_2 induced by Aβ. H_2O_2 is known to be membrane

permeable and to act as a second messenger (Almasalmeh et al., 2014; Ding et al., 2008; Forman et al., 2004; Gill and Levine, 2013; Lee et al., 2011). Generation of H_2O_2 was shown to precede loss of ΔΨ and CytC release during apoptosis (Luo et al., 2012; Tada-Oikawa et al., 1999), suggesting that the observed effects of MTZ on the inhibition of H_2O_2 production induced by Aβ could be instrumental to reduce mitochondrial dysfunction and cell death in AD. The membrane permeable properties of hydrogen peroxide and its ability to escape the cellular environment also explain our findings showing changes in the release of H_2O_2 by mitochondria isolated from Aβ-treated cells, coexisting with the lack of significant changes in cell ROS inside whole cells (after removal of their extracellular media). The ability of MTZ to reduce H_2O_2 and prevent loss of mitochondrial Δψ which we previously observed (Fossati et al., 2013) – both associated to the inhibition of CytC release may be key mechanisms contributing to the prevention of caspase activation and the resulting apoptosis in our model.

In the present report, we show that MTZ can effectively inhibit H_2O_2 production, as well as CytC release and caspase activation not only in neuronal, but also in glial cells, decreasing the levels of active-caspase 3 in IBA-1 positive microglia in the Aβ-injected mouse brain. Although mediated by different sets of receptors, a common deleterious pathway involving oxidative stress induces neuronal death and amplifies microglial activation to drive spreading neurotoxicity (Block et al., 2007). Upon depletion of the cell's antioxidant defense, H_2O_2 could act to amplify the pro-inflammatory function of microglia. High levels of intracellular ROS might result in microglial death (predominantly by apoptosis), similar to that which occurs in phagocytes in the periphery. Accordingly, caspase 3 activation and apoptosis were demonstrated in human microglia after metabolic stress (Ryu et al., 2003), and recent reports demonstrated that oligomeric Aβ induces microglial neurotoxicity and IL-1β processing via production of mitochondrial ROS (Parajuli et al., 2013). Increased expression of active caspase-3 was also found in microglia of postmortem AD brain, compared with controls (Burguillos et al., 2011). Indeed, whereas acute microglial over-activation is deleterious, active microglia might also be involved in neuronal maintenance, repair and possibly protection. Therefore, the ideal therapeutic approach would involve attenuation of the microglial response to levels that are no longer deleterious, rather than the elimination of the microglial response altogether (Choi et al., 2005). This seems to be the case in our model in presence of MTZ, which preserves microglial activation, as shown by IBA1 staining, while reducing the activation of caspase 3 below the threshold able to cause DNA fragmentation and cell death, as confirmed by our *in vitro* data. Inhibition of caspase activation protected against neuronal loss in several animal models of brain diseases involving activated microglia, including ischaemia/stroke, acute bacterial meningitis, and parkinsonism models (Braun et al., 1999; Burguillos et al., 2011; Cutillas et al., 1999; Schulz et al., 1998), and microglia exposed to the pro-inflammatory agent LPS failed to be toxic to neighboring neurons when caspase 3/7 were inhibited chemically or by siRNA. Thus, a pharmacological approach employing CAIs in the AD brain, achieving simultaneously inhibition of mitochondrial H_2O_2 production, CytC release and caspase activation in neuronal and glial cells without inhibiting physiological levels of microglial activation, would have the potential to prevent neurodegeneration both directly, restoring neuronal mitochondrial function, and indirectly, avoiding excessive microglial activation

and the derived neurotoxicity. Further studies in transgenic mouse models of AD are currently being performed to clarify the best treatment strategy and the long-term *in vivo* effects of CAIs in a chronic model of amyloidosis. Supporting the potential of a future translation of our approach to human therapy, after allometric scaling the concentration of CAI used in the current studies (20 mg/kg), was consistent with the human use of the drug (the human corresponding dose is 2.6 mg/kg, or 182 mg for a 70 kg person, which is consistent with the FDA approved dose for MTZ of 100 mg every 8 hours). The use of CAIs in clinical trials for cerebral edema and sleep apnea confirms the efficacy of these drugs in the brain and the safety of their systemic administration and provides established pharmacokinetics for the effect in the human brain. Furthermore, the current chronic use in glaucoma patients guarantees the tolerability of any side effects.

Conclusions

This study delineates the molecular mechanism of action of MTZ against Aβ-mediated H_2O_2 production, mitochondrial dysfunction and caspase activation in neuronal and glial cells, demonstrating the efficiency of the compound in an *in vivo* acute model of amyloid-mediated toxicity. Overall, the present findings support the potential of repurposing MTZ and analog FDA-approved CAIs as new therapeutic strategies for AD and related cerebral amyloidosis, emphasizing the importance of additional studies in this direction.

Acknowledgements

This work was supported by grants from the National Institutes of Health–NIA (NS051715, AG030539) the American Heart Association, the Alzheimer's Association, and the Blas Frangione Foundation. MES was a fellow from CIEN-Reina Sofia Foundation (Carlos III Health Institute, Spanish Ministry of Economy and Competitivity). We thank Dr. Evgeny Pavlov for his help with imaging.

References

Aamand R, et al. Enhancing effects of acetazolamide on neuronal activity correlate with enhanced visual processing ability in humans. Neuropharmacology. 2011; 61:900–8. [PubMed: 21736887]

Almasalmeh A, et al. Structural determinants of the hydrogen peroxide permeability of aquaporins. FEBS J. 2014; 281:647–56. [PubMed: 24286224]

Atamna H, Frey WH 2nd. Mechanisms of mitochondrial dysfunction and energy deficiency in Alzheimer's disease. Mitochondrion. 2007; 7:297–310. [PubMed: 17625988]

Balietti M, et al. Early selective vulnerability of synapses and synaptic mitochondria in the hippocampal CA1 region of the Tg2576 mouse model of Alzheimer's disease. J Alzheimers Dis. 2013; 34:887–96. [PubMed: 23313923]

Bashir M, et al. beta-Amyloid-evoked apoptotic cell death is mediated through MKK6-p66shc pathway. Neuromolecular Med. 2014; 16:137–49. [PubMed: 24085465]

Beal MF. Oxidative damage as an early marker of Alzheimer's disease and mild cognitive impairment. Neurobiol Aging. 2005; 26:585–6. [PubMed: 15708432]

Bickler PE, et al. Effects of acetazolamide on cerebral acid-base balance. J Appl Physiol (1985). 1988; 65:422–7. [PubMed: 3136134]

Block ML, et al. Microglia-mediated neurotoxicity: uncovering the molecular mechanisms. Nat Rev Neurosci. 2007; 8:57–69. [PubMed: 17180163]

Braun JS, et al. Neuroprotection by a caspase inhibitor in acute bacterial meningitis. Nat Med. 1999; 5:298–302. [PubMed: 10086385]

Burguillos MA, et al. Caspase signalling controls microglia activation and neurotoxicity. Nature. 2011; 472:319–24. [PubMed: 21389984]

Calkins MJ, et al. Impaired mitochondrial biogenesis, defective axonal transport of mitochondria, abnormal mitochondrial dynamics and synaptic degeneration in a mouse model of Alzheimer's disease. Hum Mol Genet. 2011; 20:4515–29. [PubMed: 21873260]

Chang YJ, Chen YR. The coexistence of an equal amount of Alzheimer's amyloid-beta 40 and 42 forms structurally stable and toxic oligomers through a distinct pathway. FEBS J. 2014; 281:2674–87. [PubMed: 24720730]

Choi SH, et al. Inhibition of thrombin-induced microglial activation and NADPH oxidase by minocycline protects dopaminergic neurons in the substantia nigra in vivo. J Neurochem. 2005; 95:1755–65. [PubMed: 16219027]

Cruz L, et al. Solvent and mutation effects on the nucleation of amyloid beta-protein folding. Proc Natl Acad Sci U S A. 2005; 102:18258–63. [PubMed: 16339896]

Cutillas B, et al. Caspase inhibition protects nigral neurons against 6-OHDA-induced retrograde degeneration. Neuroreport. 1999; 10:2605–8. [PubMed: 10574377]

D'Amelio M, et al. Caspase-3 triggers early synaptic dysfunction in a mouse model of Alzheimer's disease. Nat Neurosci. 2011; 14:69–76. [PubMed: 21151119]

de Calignon A, et al. Caspase activation precedes and leads to tangles. Nature. 2010; 464:1201–4. [PubMed: 20357768]

Ding Y, et al. Endogenous hydrogen peroxide regulates glutathione redox via nuclear factor erythroid 2-related factor 2 downstream of phosphatidylinositol 3-kinase during muscle differentiation. Am J Pathol. 2008; 172:1529–41. [PubMed: 18458092]

Du H, et al. Early deficits in synaptic mitochondria in an Alzheimer's disease mouse model. Proc Natl Acad Sci U S A. 2010; 107:18670–5. [PubMed: 20937894]

Duffy AM, et al. A selective role for ARMS/Kidins220 scaffold protein in spatial memory and trophic support of entorhinal and frontal cortical neurons. Exp Neurol. 2011; 229:409–20. [PubMed: 21419124]

Eckert A, et al. Mitochondrial dysfunction, apoptotic cell death, and Alzheimer's disease. Biochem Pharmacol. 2003a; 66:1627–34. [PubMed: 14555243]

Eckert A, et al. Increased apoptotic cell death in sporadic and genetic Alzheimer's disease. Ann N Y Acad Sci. 2003b; 1010:604–9. [PubMed: 15033800]

Forman HJ, et al. Redox signaling: thiol chemistry defines which reactive oxygen and nitrogen species can act as second messengers. Am J Physiol Cell Physiol. 2004; 287:C246–56. [PubMed: 15238356]

Fossati S, et al. Differential activation of mitochondrial apoptotic pathways by vasculotropic amyloid-beta variants in cells composing the cerebral vessel walls. FASEB J. 2010; 24:229–41. [PubMed: 19770225]

Fossati S, et al. Insights into Caspase-Mediated Apoptotic Pathways Induced by Amyloid-beta in Cerebral Microvascular Endothelial Cells. Neurodegenerative Diseases. 2012a; 10:324–328. [PubMed: 22156599]

Fossati S, et al. TRAIL death receptors DR4 and DR5 mediate cerebral microvascular endothelial cell apoptosis induced by oligomeric Alzheimer's Abeta. Cell Death Dis. 2012b; 3:e321. [PubMed: 22695614]

Fossati S, et al. Differential contribution of isoaspartate post-translational modifications to the fibrillization and toxic properties of amyloid-beta and the asparagine 23 Iowa mutation. Biochem J. 2013

Friedlander RM. Apoptosis and caspases in neurodegenerative diseases. N Engl J Med. 2003; 348:1365–75. [PubMed: 12672865]

Giacomotto J, et al. Evaluation of the therapeutic potential of carbonic anhydrase inhibitors in two animal models of dystrophin deficient muscular dystrophy. Hum Mol Genet. 2009; 18:4089–101. [PubMed: 19648295]

Gill T, Levine AD. Mitochondria-derived hydrogen peroxide selectively enhances T cell receptor-initiated signal transduction. J Biol Chem. 2013; 288:26246–55. [PubMed: 23880762]

Grossmann WM, Koeberle B. The dose-response relationship of acetazolamide on the cerebral blood flow in normal subjects. Cerebrovasc Dis. 2000; 10:65–9. [PubMed: 10629349]

Jiang X, Wang X. Cytochrome c promotes caspase-9 activation by inducing nucleotide binding to Apaf-1. J Biol Chem. 2000; 275:31199–203. [PubMed: 10940292]

Kim HE, et al. Formation of apoptosome is initiated by cytochrome c-induced dATP hydrolysis and subsequent nucleotide exchange on Apaf-1. Proc Natl Acad Sci U S A. 2005; 102:17545–50. [PubMed: 16251271]

Kim J, et al. Beta-amyloid oligomers activate apoptotic BAK pore for cytochrome c release. Biophys J. 2014; 107:1601–8. [PubMed: 25296312]

Lee S, et al. Mitochondrial H2O2 generated from electron transport chain complex I stimulates muscle differentiation. Cell Res. 2011; 21:817–34. [PubMed: 21445095]

Luo P, et al. Protective effect of Homer 1a against hydrogen peroxide-induced oxidative stress in PC12 cells. Free Radic Res. 2012; 46:766–76. [PubMed: 22435683]

Marques CA, et al. Neurotoxic mechanisms caused by the Alzheimer's disease-linked Swedish amyloid precursor protein mutation: oxidative stress, caspases, and the JNK pathway. J Biol Chem. 2003; 278:28294–302. [PubMed: 12730216]

Modi KK, et al. A physically-modified saline suppresses neuronal apoptosis, attenuates tau phosphorylation and protects memory in an animal model of Alzheimer's disease. PLoS One. 2014; 9:e103606. [PubMed: 25089827]

Moreira PI, et al. Mitochondrial dysfunction is a trigger of Alzheimer's disease pathophysiology. Biochim Biophys Acta. 2010a; 1802:2–10. [PubMed: 19853658]

Moreira PI, et al. Mitochondria: a therapeutic target in neurodegeneration. Biochim Biophys Acta. 2010b; 1802:212–20. [PubMed: 19853657]

Parajuli B, et al. Oligomeric amyloid beta induces IL-1beta processing via production of ROS: implication in Alzheimer's disease. Cell Death Dis. 2013; 4:e975. [PubMed: 24357806]

Price KA, et al. Altered synaptic structure in the hippocampus in a mouse model of Alzheimer's disease with soluble amyloid-beta oligomers and no plaque pathology. Mol Neurodegener. 2014; 9:41. [PubMed: 25312309]

Ryu JK, et al. Microglial activation and cell death induced by the mitochondrial toxin 3-nitropropionic acid: in vitro and in vivo studies. Neurobiol Dis. 2003; 12:121–32. [PubMed: 12667467]

Saito Y, et al. Molecular mechanisms of 6-hydroxydopamine-induced cytotoxicity in PC12 cells: involvement of hydrogen peroxide-dependent and -independent action. Free Radic Biol Med. 2007; 42:675–85. [PubMed: 17291991]

Santos RX, et al. Mitochondrial DNA oxidative damage and repair in aging and Alzheimer's disease. Antioxid Redox Signal. 2013; 18:2444–57. [PubMed: 23216311]

Schulz JB, et al. Extended therapeutic window for caspase inhibition and synergy with MK-801 in the treatment of cerebral histotoxic hypoxia. Cell Death Differ. 1998; 5:847–57. [PubMed: 10203688]

Shah GN, et al. High glucose-induced mitochondrial respiration and reactive oxygen species in mouse cerebral pericytes is reversed by pharmacological inhibition of mitochondrial carbonic anhydrases: Implications for cerebral microvascular disease in diabetes. Biochem Biophys Res Commun. 2013a; 440:354–8. [PubMed: 24076121]

Shah GN, et al. Pharmacological inhibition of mitochondrial carbonic anhydrases protects mouse cerebral pericytes from high glucose-induced oxidative stress and apoptosis. J Pharmacol Exp Ther. 2013b; 344:637–45. [PubMed: 23249625]

Smale G, et al. Evidence for apoptotic cell death in Alzheimer's disease. Exp Neurol. 1995; 133:225–30. [PubMed: 7544290]

Solesio ME, et al. The mitochondria-targeted anti-oxidant MitoQ reduces aspects of mitochondrial fission in the 6-OHDA cell model of Parkinson's disease. Biochim Biophys Acta. 2013a; 1832:174–82. [PubMed: 22846607]

Solesio ME, et al. 3-Nitropropionic acid induces autophagy by forming mitochondrial permeability transition pores rather than activating the mitochondrial fission pathway. Br J Pharmacol. 2013b; 168:63–75. [PubMed: 22509855]

Solito R, et al. Dutch and Arctic mutant peptides of beta amyloid(1-40) differentially affect the FGF-2 pathway in brain endothelium. Exp Cell Res. 2009; 315:385–95. [PubMed: 19061884]

Stadelmann C, et al. Activation of caspase-3 in single neurons and autophagic granules of granulovacuolar degeneration in Alzheimer's disease. Evidence for apoptotic cell death. Am J Pathol. 1999; 155:1459–66. [PubMed: 10550301]

Swerdlow RH, et al. The Alzheimer's disease mitochondrial cascade hypothesis. J Alzheimers Dis. 2010; 20(Suppl 2):S265–79. [PubMed: 20442494]

Tada-Oikawa S, et al. Generation of hydrogen peroxide precedes loss of mitochondrial membrane potential during DNA alkylation-induced apoptosis. FEBS Lett. 1999; 442:65–9. [PubMed: 9923606]

Viana RJ, et al. Tauroursodeoxycholic acid prevents E22Q Alzheimer's Abeta toxicity in human cerebral endothelial cells. Cell Mol Life Sci. 2009; 66:1094–104. [PubMed: 19189048]

Walsh DM, et al. Amyloid beta-protein fibrillogenesis. Structure and biological activity of protofibrillar intermediates. J Biol Chem. 1999; 274:25945–52. [PubMed: 10464339]

Wang X, et al. Methazolamide and melatonin inhibit mitochondrial cytochrome C release and are neuroprotective in experimental models of ischemic injury. Stroke. 2009; 40:1877–85. [PubMed: 19299628]

Wang X, et al. Minocycline inhibits caspase-independent and -dependent mitochondrial cell death pathways in models of Huntington's disease. Proc Natl Acad Sci U S A. 2003; 100:10483–7. [PubMed: 12930891]

Wang X, et al. Inhibitors of cytochrome c release with therapeutic potential for Huntington's disease. J Neurosci. 2008; 28:9473–85. [PubMed: 18799679]

Wright A, et al. High hopes at high altitudes: pharmacotherapy for acute mountain sickness and high-altitude cerebral and pulmonary oedema. Expert Opin Pharmacother. 2008; 9:119–27. [PubMed: 18076343]

Wu KL, et al. Loss of neuronal protein expression in mouse hippocampus after irradiation. J Neuropathol Exp Neurol. 2010; 69:272–80. [PubMed: 20142763]

Xie H, et al. Mitochondrial alterations near amyloid plaques in an Alzheimer's disease mouse model. J Neurosci. 2013; 33:17042–51. [PubMed: 24155308]

Zhou Q, et al. Rotenone Induction of Hydrogen Peroxide Inhibits mTOR-mediated S6K1 and 4E-BP1/eIF4E Pathways, Leading to Neuronal Apoptosis. Toxicol Sci. 2014

Zhu CL, et al. [Cytochrome C release and apoptosis in neonatal rat cerebral hypoxia-ischemia]. Zhonghua Er Ke Za Zhi. 2004; 42:437–40. [PubMed: 15265431]

Zhu S, et al. Minocycline inhibits cytochrome c release and delays progression of amyotrophic lateral sclerosis in mice. Nature. 2002; 417:74–8. [PubMed: 11986668]

Zussy C, et al. Alzheimer's disease related markers, cellular toxicity and behavioral deficits induced six weeks after oligomeric amyloid-beta peptide injection in rats. PLoS One. 2013; 8:e53117. [PubMed: 23301030]

Highlights

- Methazolamide (MTZ) prevents neuronal and glial Aβ-mediated apoptosis
- MTZ inhibits Aβ toxicity through modulation of mitochondrial H_2O_2 production
- Cytochrome C release, caspase-9 and -3 activation are all prevented by MTZ
- Intrahippocampal Aβ Injection in mice causes neuronal loss and glial activation
- MTZ prevents caspase 3 activation and neuronal loss after hippocampal Aβ injection

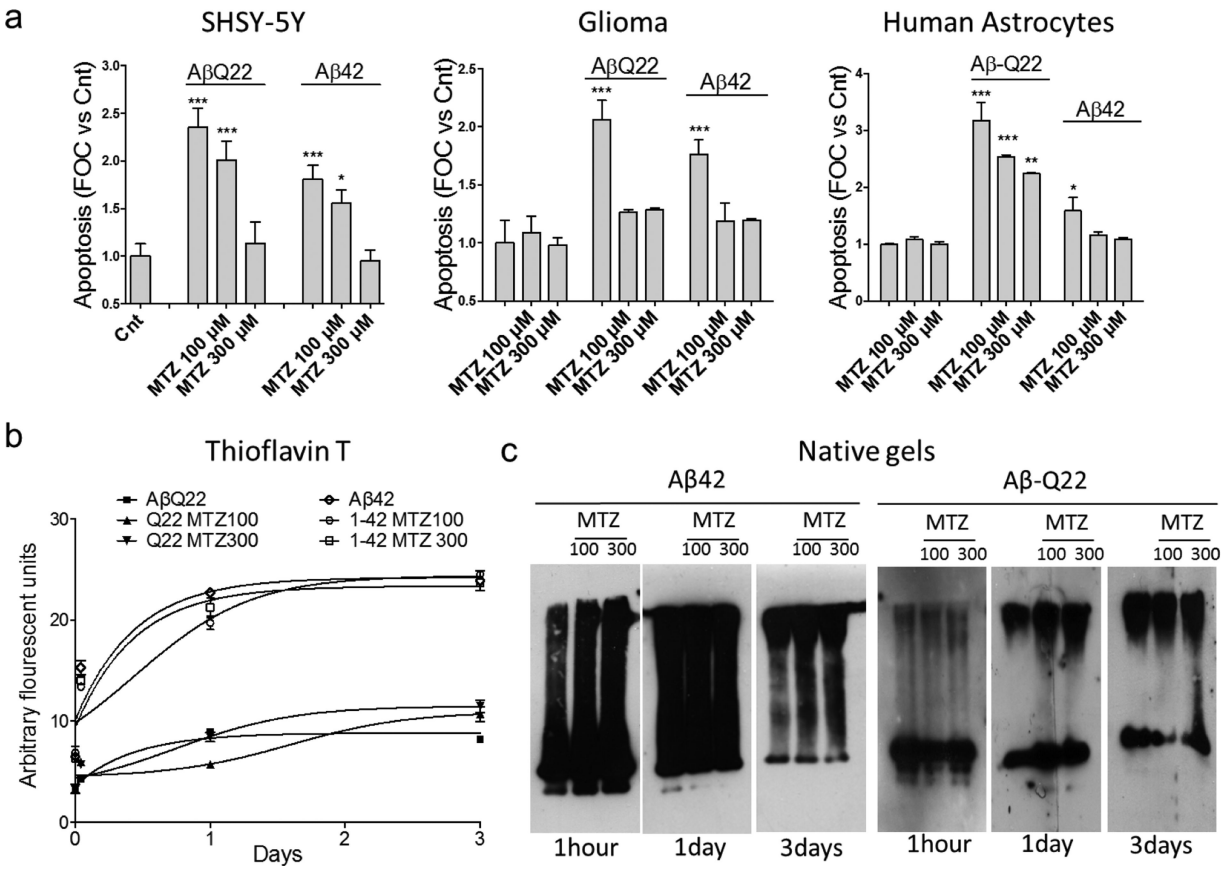

Figure 1. Methazolamide prevents DNA fragmentation in neuronal and glial cells without affecting Aβ aggregation

a) Cultures of neuronal SHSY-5Y cells, glioma cells and normal human astrocytes were challenged with 50 μM Aβ40-Q22 or 10 μM Aβ42, in presence or absence of methazolamide (MTZ) 100 or 300μM. Apoptosis was evaluated as presence of fragmented nucleosomes by Cell Death Detection ELISA^{plus} after 1 day in SHSY-5Y cells and astrocytes and after 3 days in glioma cells. Results are expressed as fold of change compared with no-peptide controls (Cnt). Data are representative of at least three independent experiments performed in duplicate. Bars represent means +/− S.D. *P <0.05, **P<0.001, ***P<0.0001 compared to Cnt cells in absence of peptides and MTZ. **b)** Thioflavin T binding of Aβ42 and Aβ40-Q22 (both aggregated at 50μM concentration for up to 3 days) in presence or absence of MTZ (100μM or 300μM). Fluorescence evaluation (excitation 435 nm/emission 490 nm) of Thioflavin T at different time points during peptide aggregation was performed as described in Materials and Methods. Thioflavin T binding, indicating peptide oligomerization/ fibrillization was not significantly affected by MTZ. Data is representative of experiments performed 3 times in duplicate. **c)** Native Western Blotting analysis. Aβ peptides were aggregated for different time points (1 hour, 1 day and 3 days) in presence or absence of MTZ. Samples were separated in non-denaturing 5–30% gradient gels, electrotransferred to nitrocellulose, and probed with an antibody recognizing Aβ. Electrophoretic mobility at each aggregation time point was not affected by the presence of MTZ. Data are representative of 3 different experiments.

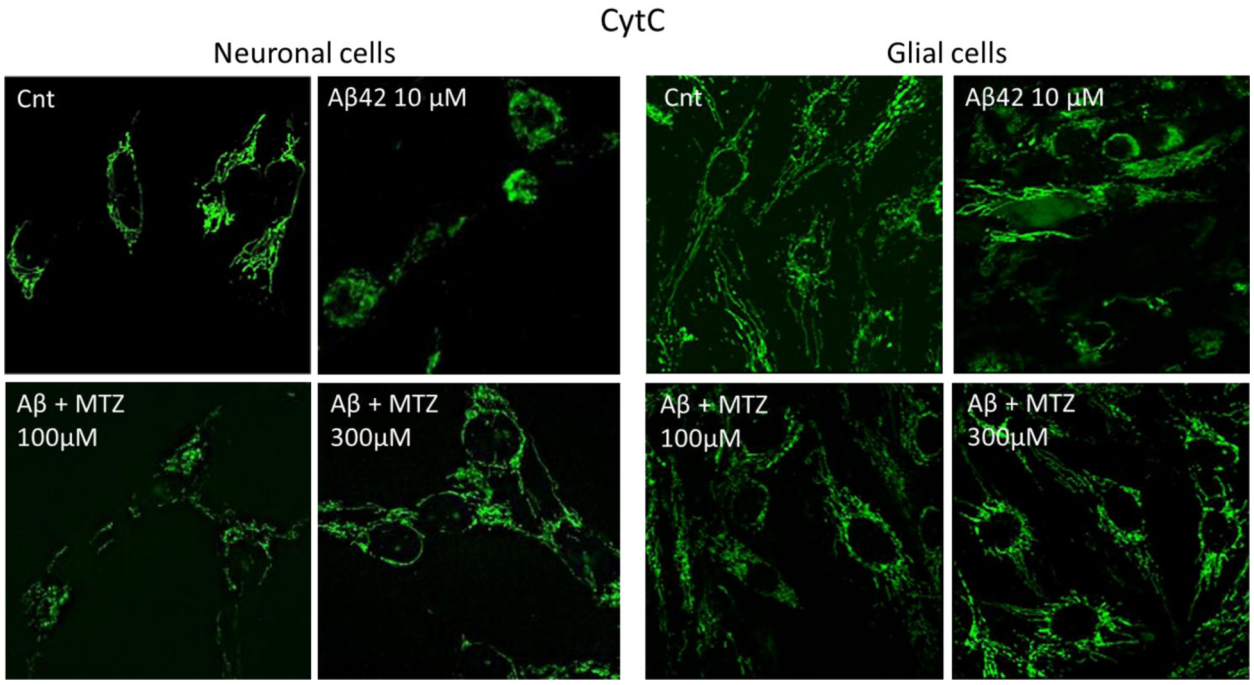

Figure 2. Methazolamide inhibits mitochondrial CytC release in neuronal and glial cells challenged with Aβ

Neuronal SHSY-5Y (left panel) and Glioma cells (right panel) were challenged with 10 μM Aβ42 for 24 hours. Green fluorescence highlights CytC staining; chain-like appearance of CytC represents mitochondrial localization, whereas more diffuse green staining indicates release into the cytoplasm. Magnification 40X. Cnt = control cells in absence of peptide and MTZ. Images are representative of 3 independent experiments.

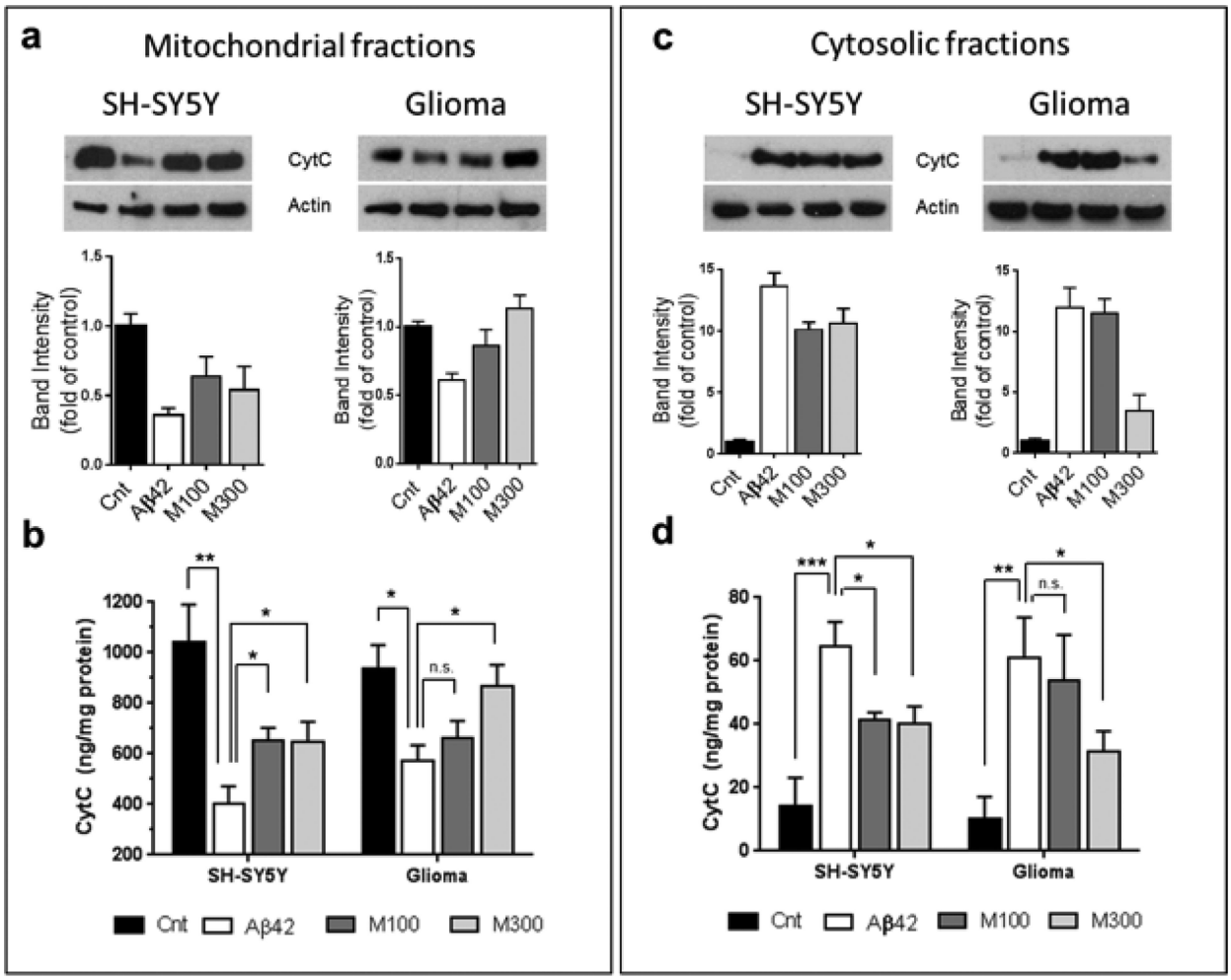

Figure 3. Evaluation of the preventive effect of MTZ on Aβ-mediated mitochondrial CytC release by Western blot and ELISA

Neuronal SH-SY5Y and glioma cells were challenged with Aβ42 (10 μM; 24h) in the presence or absence of MTZ (100 and 300 μM) and subsequently subjected to subcellular fractionation. CytC was evaluated in mitochondrial and cytosolic extracts by WB and ELISA. **(a-c)** Western blot analysis of mitochondrial **(a)** and cytosolic **(c)** extracts. After electrophoretic separation of the respective subcellular fractions and electrotransfer to PVDF, membranes were probed for CytC and β-actin as loading control. Band intensities after normalization to the respective loading controls are illustrated in the bar-graphs below the corresponding WB. Each WB is representative of duplicate independent experiments. **(b-d)** CytC quantitated by ELISA in the mitochondrial **(b)** and cytoplasmic **(d)** extracts. Bars represent mean ± SD of triplicate experiments. * indicates $p<0.05$, ** $p<0.01$, and *** indicates $p<0.001$

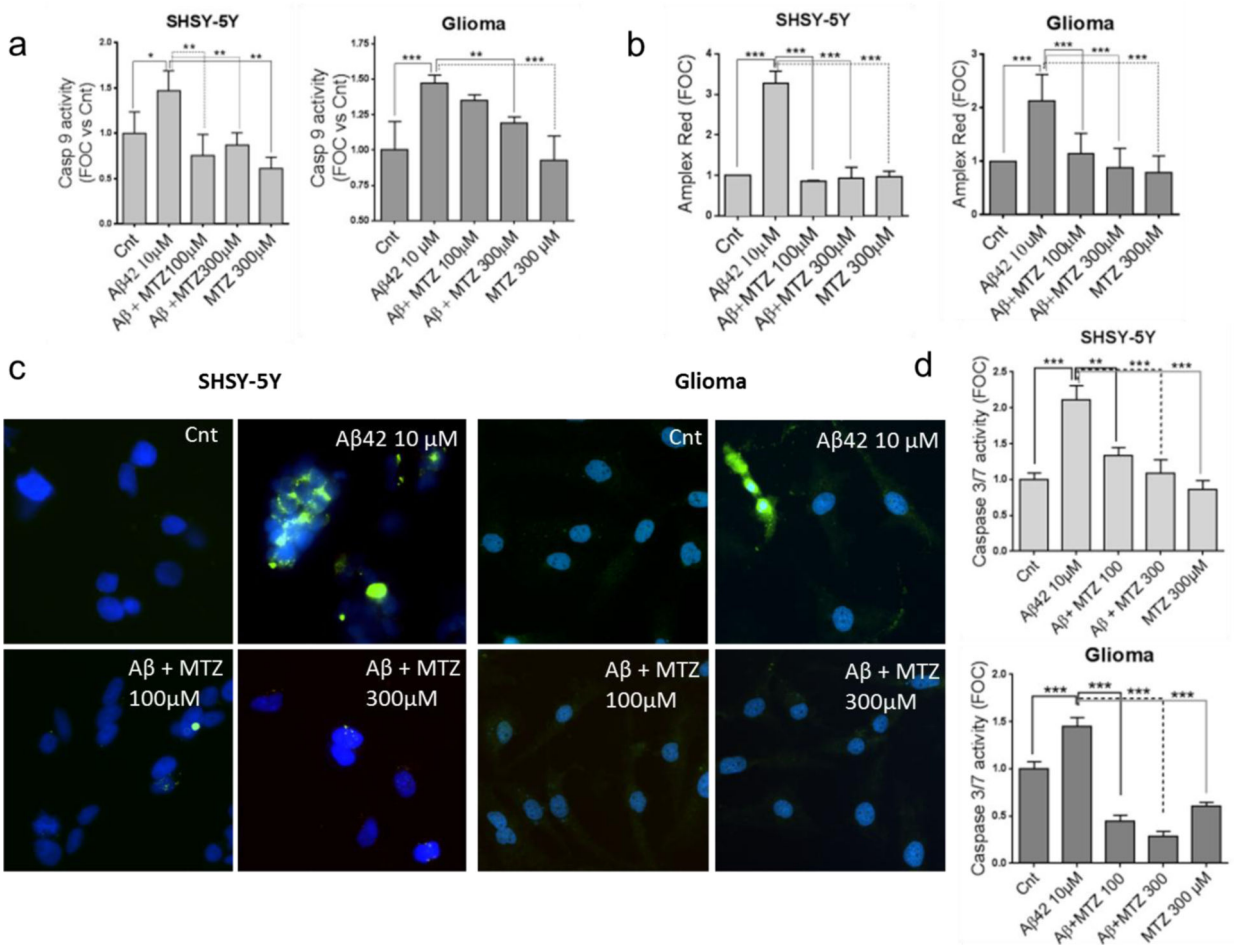

Figure 4. Effect of MTZ on Aβ-mediated caspase activation and H_2O_2 production

a) Caspase 9 activity in neuronal and glial cells was measured by luminescence. MTZ inhibited the activation of caspase 9 induced by incubation with 10μM Aβ42 for 24 hours in both cell types. **b)** Mitochondria were isolated after cell treatment with Aβ42 in presence or absence of MTZ, and mitochondrial H_2O_2 production was quantified using Amplex Red Hydrogen Peroxidase/Peroxidase Assay as specified in Methods. Results are expressed as fold change in H_2O_2 production compared with no-peptide controls (Cnt). **c)** MTZ inhibited Aβ-mediated caspase 3 activation, visualized by anti-active caspase 3 staining after 24 hours treatment with 10 μM Aβ42. Green fluorescence highlights cells presenting active caspase 3. Nuclei were stained in blue with DAPI. Magnification: 20X. **d)** Caspase 3/7 activity in neuronal and glial cells was measured by luminescence. MTZ inhibited the activation of caspase 3/7 after 24 hours in both cell types. For **a**, **b** and **c**, and **d**, data are representative of at least three independent experiments performed in duplicate. Bars represent means +/− S.D. * P <0.05, ** P<0.01, *** P<0.0001.

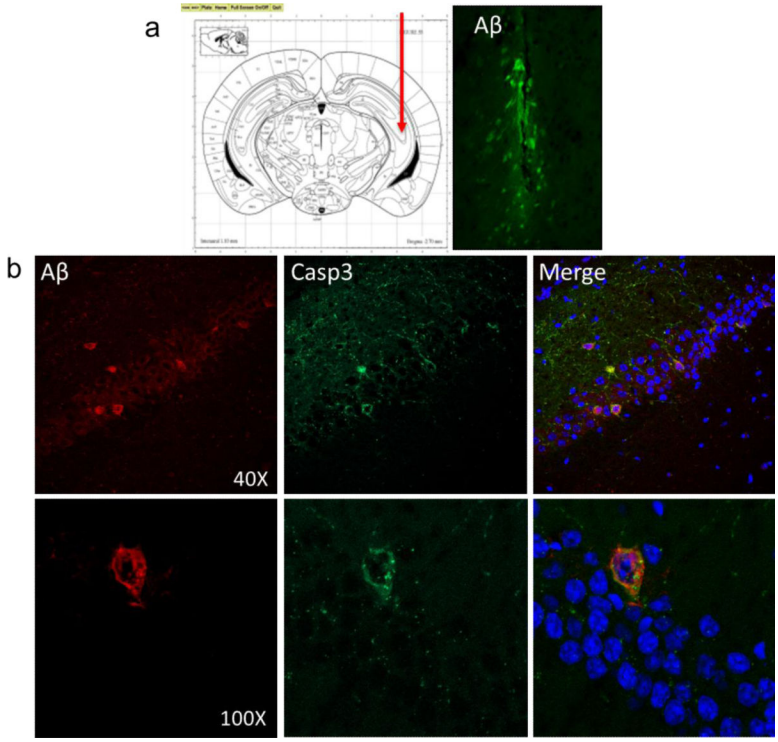

Figure 5. Hippocampal injection of Aβ induces caspase activation in Aβ-positive CA1 cells

a) Intra-hippocampal Aβ injection in mice was performed as described in Material and Methods. The site of injection is visualized as a red arrow in the Paxinos and Franklin Coordinates Atlas in the left panel. Immunohistochemical staining of Aβ was visualized as green fluorescence 1 hour after injection (right panel), and highlights both cellular and parenchymal localization of the peptide around the injection site. **b)** Immunohistochemical analysis of the ipsolateral CA1 hippocampal region 4 hours after Aβ injection. Red fluorescence represents Aβ, while green fluorescence highlights active caspase 3. Nuclei were stained in blue with To-Pro. Active caspase 3 staining colocalized specifically with CA1 hippocampal cells containing internalized Aβ. Top panels: 40X magnification. Bottom panels: 100X magnification. Results are representative of 5 injected mice.

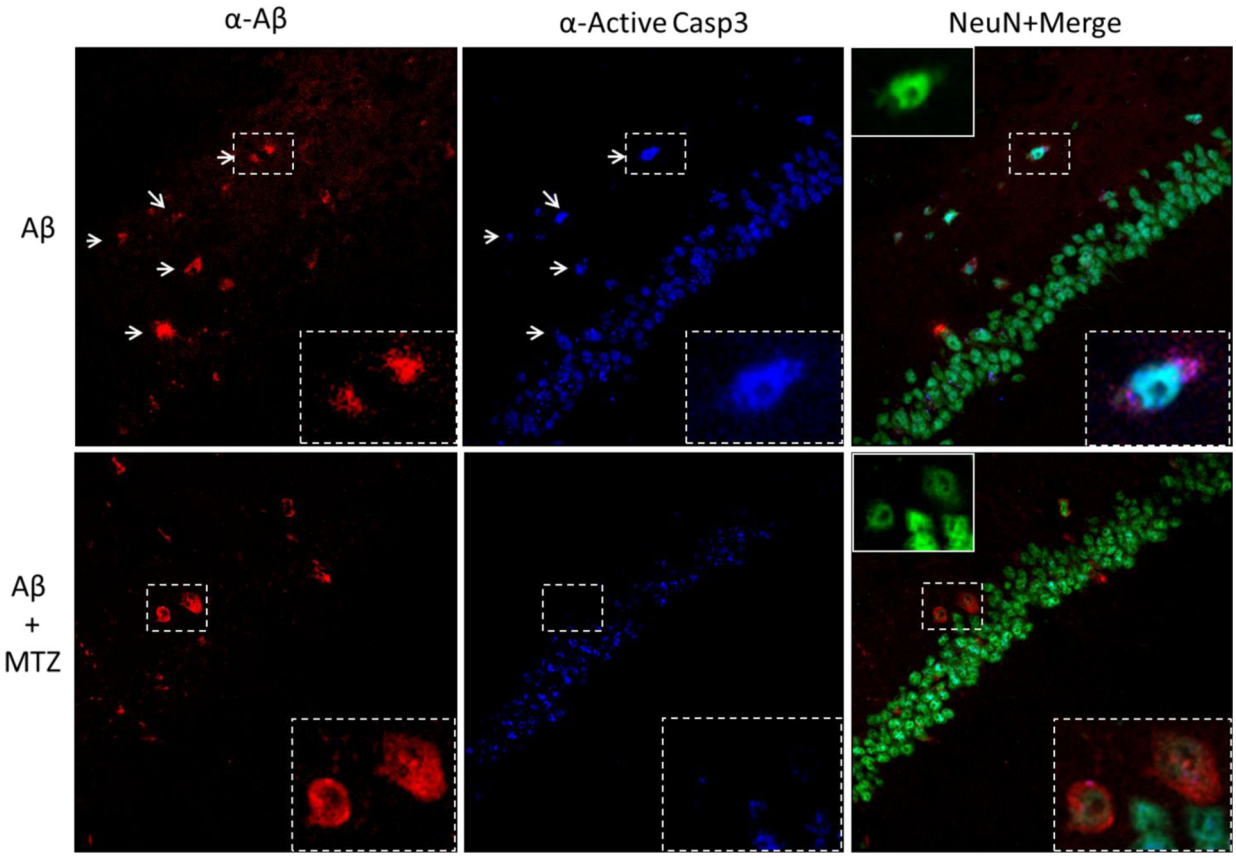

Figure 6. MTZ inhibits caspase 3 activation in hippocampal neurons presenting internalized Aβ

Aβ was stained in red, active caspase 3 in blue and neurons were visualized in green by NeuN. In absence of MTZ treatment, CA1 neurons with internalized Aβ presented active caspase 3 staining, as in Fig 4. Arrows highlight cells showing both Aβ and active caspase 3. In mice treated with MTZ, Aβ-positive neurons did not present caspase 3 activation. Inserts delimited by the dashed line represent magnifications of neurons, and show colocalization of caspase 3 with Aβ in absence of MTZ (top panels), or lack of active caspase 3 in Aβ positive neurons for MTZ treated mice (bottom panels). Inserts delimited by the continuous line in the right panels represent NeuN staining of the magnified neurons. Main image: 40X magnification. Inserts: 100X. Results are representative of staining performed in 5 MTZ-treated and 5 untreated mice.

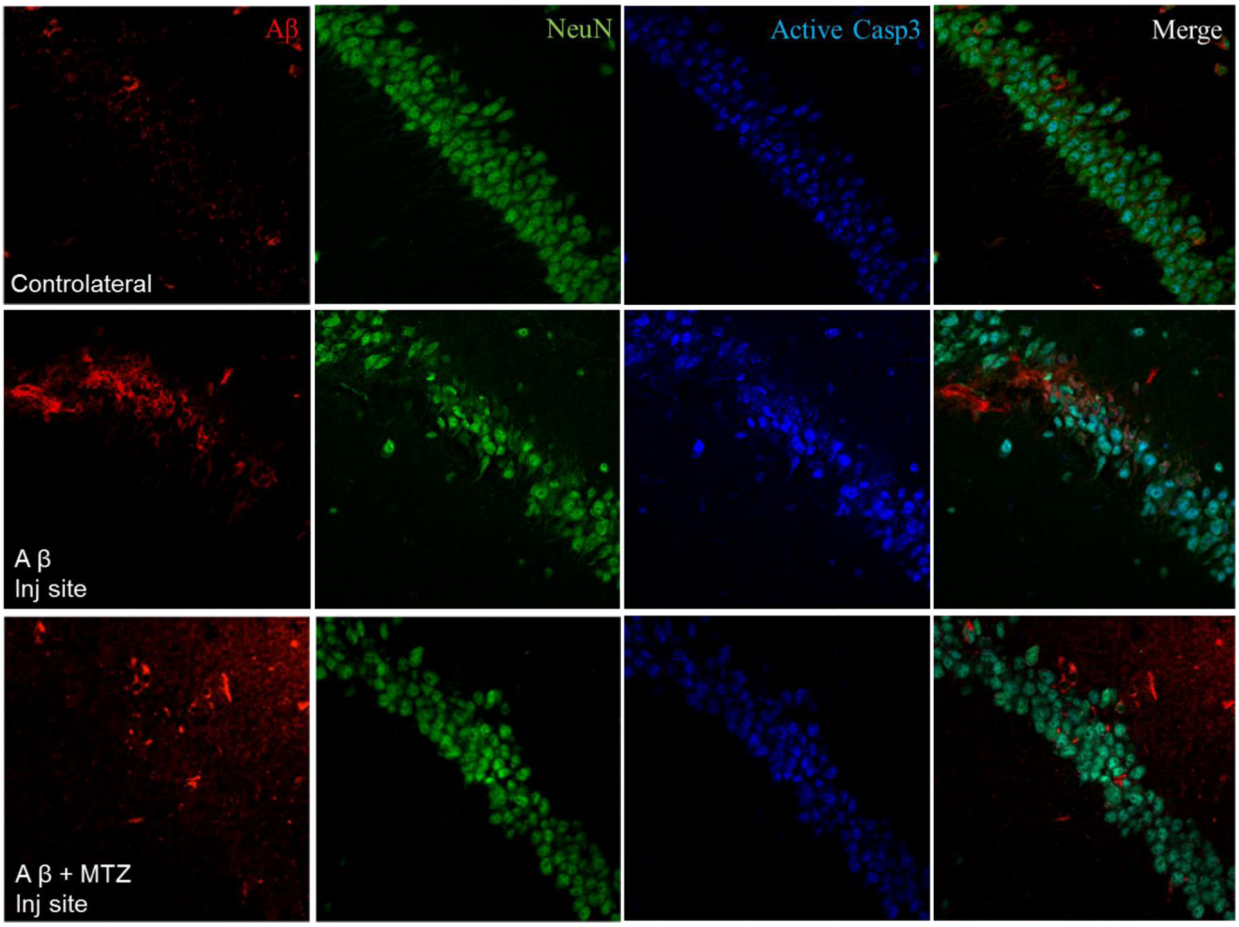

Figure 7. Effect of MTZ on hippocampal neurodegeneration and caspase 3 activation at the injection site

Immunostaining performed in a region of the hippocampus in close proximity to the injection site (≈ 100 μm) in mice injected with Aβ in presence or absence of IP injection of MTZ, and sacrificed after 4 hours. Aβ is stained in red, active caspase 3 in blue, and neurons are stained in green by NeuN. The top panels, used as control, represent the contralateral hippocampus in a mouse injected with Aβ. In the middle panels, neurodegeneration in proximity of the injection site is visualized as loss of NeuN-positive neuronal bodies around the site of Aβ injection compared to the contralateral hemisphere, and is prevented by MTZ (bottom panels). The increase in caspase 3 activation induced by Aβ around the injection site is also inhibited in mice treated with MTZ. N ≥ 4 mice per group.

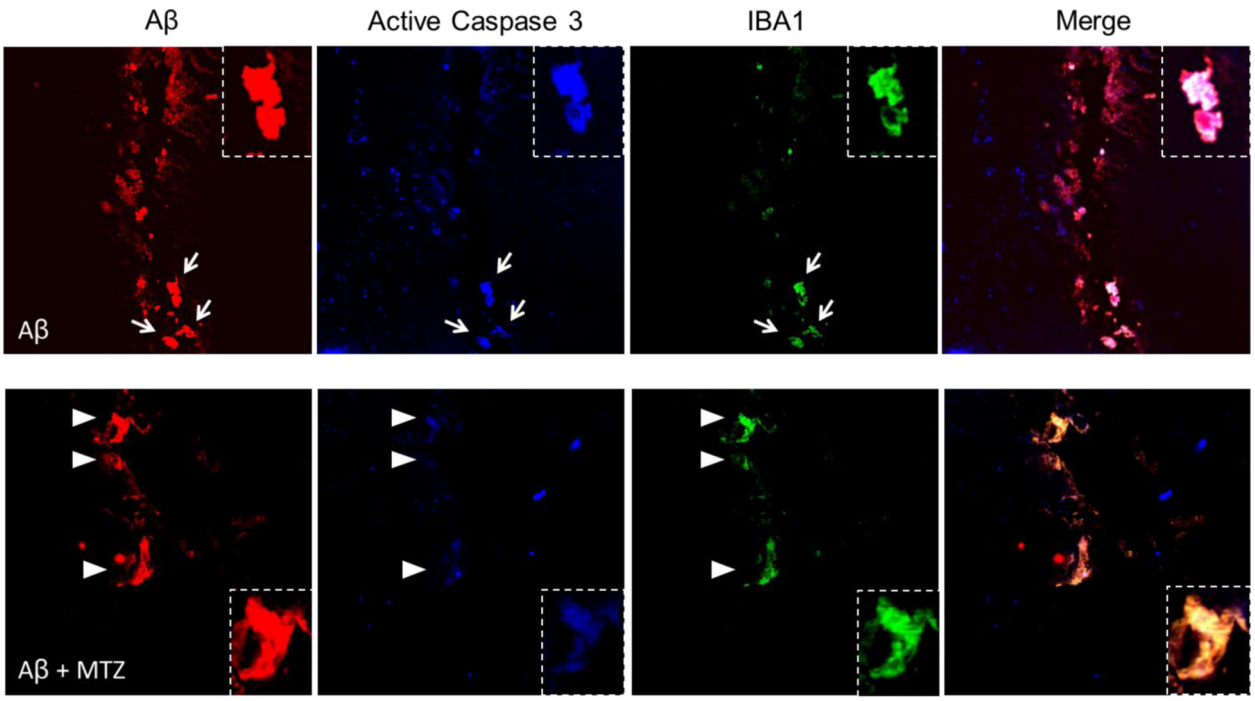

Figure 8. Effect of MTZ on caspase 3 activation in reactive microglia around the injection site

Staining at the injection site shows Aβ in red, active caspase 3 in blue and reactive microglia, stained by IBA1, in green. Some of the cells internalizing Aβ at the injection site can be identified as active microglia in both MTZ-treated and untreated mice, based on IBA1 reactivity and ameboid shape. Reactive microglia, positive for IBA1 and presenting internalized Aβ, shows caspase 3 activation in absence of MTZ treatment (top panels, arrows), while IBA1-positive microglia presents a reduced staining for active-caspase 3 in mice injected with MTZ (bottom panels, arrowheads). Notably, the color merge appears white (cells positive for Aβ, IBA1 and active-caspase 3) in Aβ-injected mice, while it's yellow (merge of IBA1 and Aβ) in mice treated with MTZ before peptide injection.

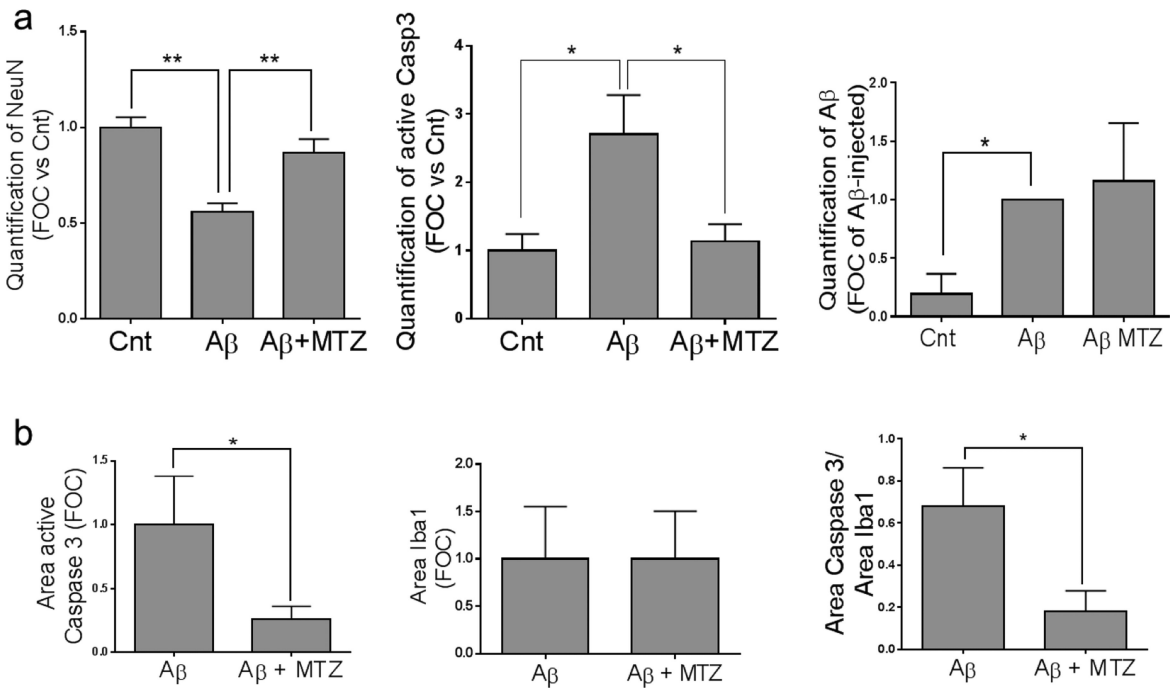

Figure 9. Quantitative evaluation of the protective effect of MTZ in the in vivo experiments

Mice were intracerebrally injected with Aβ in the presence or absence of MTZpre-treatment as described in Methods**.** Total areas highlighted by each specific staining in proximity of the injection site were quantitated with the aid of Image J, and are represented in the graphs. **a)** Aβ inoculation causes loss of hippocampal NeuN staining in comparison with the contralateral site, a decrease not observed in MTZ-treated mice (left panel). Aβ inoculation also induces neuronal caspase 3 activation, which is prevented by MTZ (central panel). Aβ staining, which is negligible in the contralateral (Cnt) hemisphere, is unaffected by MTZ (right panel). **b)** Quantification of active caspase 3 and IBA1 staining, as well as the ratio between active caspase 3 and IBA1 staining in microglia are represented in the left, central and right panels, respectively. For all experiments, signal, quantification was performed in brain slices of 3 or more different animals. * indicates $p<0.05$; ** indicates $p<0.01$.